Investigational New Drugs (2019) 37:961–972
https://doi.org/10.1007/s10637-018-00718-8

PRECLINICAL STUDIES

Biodistribution, pharmacokinetics and radioimmunotherapy of ^{188}Re-cetuximab in NCI-H292 human lung tumor-bearing nude mice

Ya-Jen Chang[1] · Chung-Li Ho[1] · Kai-Hung Cheng[1] · Wan-I Kuo[1] · Wan-Chi Lee[1] · Keng-Li Lan[2,3] · Chih-Hsien Chang[1]

Received: 5 November 2018 / Accepted: 25 December 2018 / Published online: 5 January 2019

Summary

Background Cetuximab is a fully humanized IgG1 subclass monoclonal that binds specifically to the human epidermal growth factor receptor (EGFR). Although EGFR is expressed in normal cells, the overexpression of EGFR is detected in many human cancers, such as colon, rectum and lung tumors. In this study, cetuximab with a combination of radiotherapy nuclear ^{188}Re achieved better therapeutic effect on lung cancer. *Methods* ^{188}Re-cetuximab administered by the i.v. route in human NCI-H292 lung tumor-bearing mice was investigated. NanoSPECT/CT images were taken to evaluate the distribution and tumor targeting of ^{188}Re-cetuximab in mice. The anti-tumor effect of ^{188}Re-cetuximab was assessed by the tumor growth inhibition, survival ratio. *Results* For nanoSPECT/CT imaging, a significant uptake in tumor was observed at 24 and 48 h following the injection of ^{188}Re-cetuximab. The anti-tumor effect of ^{188}Re-cetuximab was assessed by tumor growth inhibition and the survival ratio. The tumor-bearing mice treated with ^{188}Re-cetuximab showed a better mean tumor growth inhibition rate (MGI = 0.049) and longer median survival time and lifespan (62.50 d; 70.07%) than those treated with ^{188}Re-perrhenate and cetuximab only by single injection. A synergistic effect of tumor growth inhibition was observed with the combination index exceeding one for ^{188}Re-cetuximab (CI = 6.135 and 9.276). *Conclusion* The tumor targeting and localization of 188Re-cetuximab were confirmed in this study. Synergistic therapeutic efficacy was demonstrated for the radioimmunotherapy of ^{188}Re-cetuximab. The results of this study reveal the potential advantage and benefit obtained from ^{188}Re-cetuximab for diagnosis and therapy of oncology applications in the future.

Keywords ^{188}Re · Cetuximab · Radioimmunotherapy

Abbreviations

AUC	Area under the curve
CI	Combination index
Cl	Clearance
CR	Complete response
CRC	Colorectal cancer
C_{max}	The maximum concentration
EGFR	Epidermal growth factor receptor
FLEX	First-line erbitux in lung cancer
IR	Inhibition rate
mAbs	Monoclonal antibodies
MAA	Maximum administered activity
MGI	Growth inhibition rate
MTD	Maximum tolerated dose
NCA	Noncompartmental analysis
NHL	Non-Hodgkin's lymphoma
ORR	Overall response rate
RIT	Radioimmunotherapy
ROI	Region of interest
$T_{1/2z}$	Elimination half-life
VOIs	Volumes of interest

✉ Chih-Hsien Chang
chchang@iner.gov.tw

[1] Institute of Nuclear Energy Research, 1000 Wenhua Rd, Longtan District, Taoyuan City, Taiwan

[2] Division of Radiation Oncology, Department of Oncology, Taipei Veterans General Hospital, Taipei, Taiwan

[3] Institute of Traditional Medicine, School of Medicine, National Yang-Ming University, Taipei, Taiwan

Introduction

Lung cancer is the leading cause of cancer mortality worldwide [1]. The two major subtypes are small cell lung cancer (SCLC) and non-small cell lung cancer (NSCLC) [2]. NSCLC accounts for about 85% of all lung cancer cases [3]. For early stage or locally advanced lung cancer, surgery is the most

effective treatment and combined chemotherapy is the standard adjuvant approach. However, about 40% of patients with NSCLC presented with unresectable and metastatic tumors (stage IV) [4]. Since the effectiveness of current standard treatment for advanced NSCLC (i.e. chemotherapy) has reached a limit [5], a requirement for novel therapies is required in the treatment of this disease.

Antibodies can recognize specific antigens, and this feature has triggered development of monoclonal antibodies as delivery vehicles for radionuclides. Conventional external-beam radiation therapy is suited to the treatment of localized disease, whereas radioimmunotherapy offers the possibility of treating localized, metastatic, or diffuse tumors. During this period, more than 10 antibody-based pharmaceuticals have been approved for treating various diseases by the Food and Drug Administration (FDA).

Cetuximab is a chimeric human-murine monoclonal immunoglobulin antibody. It blocks ligand binding to EGFR, leading to a decrease in receptor dimerisation, autophosphorylation and activation of signaling pathways. Cetuximab may also act by means of antibody-dependent cellular cytotoxicity and complement-dependent cytotoxicity [3]. A previous clinical study showed cetuximab combined with chemotherapy significantly improved survival in patients with non-small cell lung cancer (NSCLC) compared with chemotherapy alone [6]. Several phase II trials have evaluated if cetuximab in combination with different first-line chemotherapy regimens could enhance the synergic effect. The promising efficacy results of the addition of cetuximab with cisplatin plus vinorelbine as firstline treatment in a phase II study of lung cancer (overall response rate (ORR): 35% vs. 28%) [7] led to the FLEX (First-Line Erbitux in Lung Cancer) phase III trial [6, 8]. In this phase III trial, the combination with cetuximab significantly improved overall survival compared with chemotherapy alone (cisplatin plus vinorelbine) in chemotherapy-naive patients with advanced EGFR-positive NSCLC.

Radioimmunotherapy (RIT) uses an antibody labeled with a radionuclide to deliver cytotoxic radiation to a target cell. This therapeutic strategy can significantly expand the therapeutic index of therapeutic materials by minimizing the systemic exposure and toxicity of radionuclides, simultaneously maximizing the delivery of radionuclides to the target (e.g., tumor lesion). An additional attractive feature of radioimmunotherapy is the crossfire effect, delivering radiation to unbound cells (e.g., inaccessible to antibody due to poor vascularization) and resulting in direct cytotoxicity. Radioimmunotherapy is usually performed using whole IgG mAbs (monoclonal antibodies) with a molecular weight of 150 kDa. The choice of the radionuclide depends on the size of the tumor. The nucleotide with high energy b-emitters (e.g., ^{90}Y and ^{188}Re) is suitable therapy for larger tumors, and the b-emitters nucleotide (e.g., ^{177}Lu and ^{131}I) is suitable for treating smaller tumors [9, 10]. RIT have fewer side effects than chemotherapy and has the ability to directly target and kill the cancer cells.

^{90}Y-Ibritumomab tiuxetan (Zevalin) has been approved by the US FDA in clinical usage for treatment of B cell non-Hodgkin's lymphoma [11, 12]. Yttrium-90 ibritumomab tiuxetan (Zevalin, Spectrum Pharmaceuticals, Inc.) was the first radioimmunoconjugate approved by the FDA for treating patients with non-Hodgkin's lymphoma. Zevalin was based on antibodies specific to CD20, which was an antigen that was present on normal B cells and cancerous B cell lymphomas. A clinical trial phase III study compared ^{90}Y-Ibritumomab tiuxetan with rituximab in patients with relapsed or refractory low-grade or transformed B cell Non-Hodgkin's lymphoma (NHL) [13]. The overall response rate (ORR) was 80% for the ^{90}Y-Ibritumomab tiuxetan group versus 56% for the rituximab group ($P = 0.002$), complete response (CR) rates were 30% and 16% in the ^{90}Y-Ibritumomab tiuxetan and rituximab groups ($P = 0.04$) [12].

Preclinical data indicated the anti-epidermal growth factor receptor (EGFR) agent cetuximab as a radiosensitizer for radiotherapy [14]. Inhibition of the EGFR by small molecule tyrosine kinase inhibitors (TKI), such as erlotinib, or monoclonal antibodies (mAb), such as cetuximab, has been shown to radiosensitize a limited number of non-small-cell lung carcinoma (NSCLC) and head and neck cancer (HNCC) cell lines in vitro and in vivo [15–19]. In trials, the combination of radiotherapy plus cetuximab resulted in prolonged survival in a pivotal phase III trial [20, 21].

Rhenium-188 is one of the most readily available generator derived and useful radionuclides for therapy emitting β particles (2.12 MeV, 71.1% and 1.965 MeV, 25.6%) and imageable gammas (155 keV, 15.1%). The ^{188}W/^{188}Re generator is an ideal source for the long term (4–6 months) continuous availability of no carrier added ^{188}Re is suitable for preparing radiopharmaceuticals for radionuclide therapy. The objective of the present study was to develop a novel strategy to enhance the therapeutic efficacy of cetuximab for lung cancer by co-treatment with radiotherapy and immunotherapy.

Materials and methods

Cell cultures and animal model

The NCI-H292 human lung carcinoma cell line was obtained from the American Type Culture Collection (Manassas, VA, USA). It was grown in RPMI-1640 medium supplemented with 10% (*v*/v) fetal bovine serum (FBS) and 2 mM L-glutamine at 37 °C in 5% CO_2. Cells were detached with 0.05% trypsin/0.53 mM EDTA in Hanks' Balanced Salt Solution (HBSS). Six-week-old male BALB/c mice were obtained from the National Animal Center of Taiwan (Taipei, Taiwan, ROC), with food and water provided ad libitum in the animal house of the

INER. Animal research protocols were approved by the Institutional Animal Care and Use Committee (IACUC) at the Institute of Nuclear Energy Research. Mice were subcutaneously inoculated with 2×10^6 tumor cells in the right hind flank. About 7–10 days after inoculation, the animals developed tumors of about 50–100 mm^3 in size.

Preparation of ^{188}Re-cetuximab

Five mg of cetuximab (Erbitux®) was reduced with 2-mercaptoethanol in a molar ratio of mAb:2-ME = 1:1074 and purified by size-exclusion PD MidiTrap G-25 column. MDP (1.125 mg), $SnCl_2$ (0.057 mg), ascorbic acid (0.0255 mg) and reduced cetuximab (0.2~0.6 mg) were mixed in a pre-sterilized glass vial and lyophilized for 24 h. Cetuximab were labeled with ^{188}Re using lyophilized kits containing 1.125 mg of MDP, 0.057 mg of $SnCl_2$, and 0.0255 mg of ascorbic acid. Briefly, 430~1221 MBq of ^{188}Re-perrhenate in 0.5 ml saline solution were added into a lyophilized kit and 1 N HCl was added to adjust the pH to 5.5–6. Following incubation at 37 °C for 4 h. The radiolabeling yield and radiochemical purity was checked by instant thin layer chromatography and size exclusion-HPLC analysis.

To evaluate the immunoreactivity of ^{188}Re-cetuximab, cell binding studies with ^{188}Re-cetuximab were carried out using NCI-H292 cells. Nonspecific binding was determined in the presence of 100-fold excess of cetuximab. After incubation of ^{188}Re-cetuximab with cells for 1 h, the samples were washed twice in cold PBS containing 1% bovine serum albumin. Each sample was counted in a gamma counter (WIZARD 1480, Perkin-Elmer). Cell bound radioactivity (%) was calculated by (cell bound radioactivity - nonspecific binding radioactivity)/ total radioactivity ×100.

Biodistribution and pharmacokinetic studies of ^{188}Re-cetuximab

Twenty nude mice (five mice per group) received an intravenous injection of 1.85 MBq /100 μl of ^{188}Re-cetuximab with 2.38 μg cetuximab 14 days after implanting tumors of 30–80 mm^3 in size. At various time points (4, 24, 48 and 72 h), the mice were sacrificed by CO_2 asphyxiation. Blood samples were collected through cardiac puncture. Organs of interest were removed, washed and weighed, and the radioactivity was measured with a gamma counter. The results were expressed as the percentage injected dose per gram of tissue (%ID/g).

For pharmacokinetics, eight normal nude mice received an intravenous injection of 1.85 MBq /100 μl of ^{188}Re-cetuximab with 2.38 μg cetuximab at about 8–10 weeks of age. At various time points (0.5, 1, 4, 24, 48, 72 and 168 h), mice were anesthetized by inhalation of 2–3% isoflurane and blood samples were collected through cardiac puncture. The blood samples were measured for radioactivity by gamma counter (WIZARD 1480, Perkin-Elmer) and expressed as the percentage injected dose per milliliter (%ID/ml). The pharmacokinetic parameters of ^{188}Re-cetuximab in blood were determined using the WinNonlin software version 5.3 (Pharsight Corp., Mountain View, CA). The non-compartmental analysis (NCA) was used to determine the pharmacokinetic parameters including terminal half-life ($T_{1/2}z$), Cmax, total body clearance (Cl) and area under the curve (AUC).

SPECT/CT imaging

For evaluating the distribution of 188Re-cetuximab and 188Re-human IgG (12.95 MBq/mouse) following intravenous injection, single-photon emission computed tomography (SPECT) imaging was performed with four-headed multiplexing multipinhole nanoSPECT (Bioscan Inc., Washington D.C., USA). Each head was fitted with an application-specific tungsten collimator with nine pinholes. This study used a mice aperture, comprising a total of 36 individual 1-mm diameter pinholes (nine pinholes in every collimator, $4 \times 9 = 36$) providing a maximum resolution of 0.75 mm for SPECT imaging. The nanoSPECT was calibrated with a phantom, approximately the size of the animals, filled with a known amount of ^{99m}Tc. The axial FOV was extended using a step-and-shoot helical scan of the animal, with the user defining a range from 24 to 270 mm according to the region to be imaged. The energy peak for the camera was set at 155 keV. The mice were scanned at 1, 4 and 24 h after injection of ^{188}Re-cetuximab. An acquisition time of 60 s per view was chosen. The CT imaging was performed immediately following the whole-body SPECT imaging with a 55-kVp tube voltage in 180 projections. For calculating tumor uptake value, 0.185–0.74 MBq radioactivity of ^{188}Re was used as a reference sources. SPECT images were reconstructed with HiSPECT NG software (Scivis GmbH, Germany) and fused with CT datasets using InVivoScope software (Bioscan Inc.) For image analysis, all data processing was performed using PMOD Version 3.3 (PMOD Technologies Ltd., Zurich, Switzerland). Volumes of interest (VOIs) were drawn encompassing the tumor and reference source on the corresponding CT images. The VOIs were transferred to SPECT images, and the count values of the tumor and reference source were derived. SPECT images were reconstructed with HiSPECT NG software (Scivis GmbH, Germany) and fused with CT datasets using InVivoScope software (Bioscan Inc.). Reconstructed SPECT images were reoriented and analyzed with InVivoScope software using CT data as a reference.

Dosimetry

For estimating the absorption doses in each organ and the total human body, the relative organ mass scaling method was used

[22, 23]. The uptake and doses in various tissues/organs were derived from the radioactivity concentration in tissues and organs of interest, assuming a homogeneous distribution within each source region. The calculated mean value of %IA/g for the organs in mice was extrapolated to uptake in the organs of a 70-kg adult [24, 25]. The extrapolated values (%IA) in the human organs at 4, 24, 48 and 72 h were fitted with exponential functions and integrated to obtain the number of disintegrations in the source organs; this information was input into the OLINDA/EXM computer program. The integrals (MBq-h/MBq administered) for organs were calculated and used for the dosimetry estimation.

To evaluate the recommended MAA of ^{188}Re-cetuximab for patients, the liver, kidney and spleen are common normal-organ sites of ^{188}Re-cetuximab localization and may, therefore, be dose limiting, although red marrow is most often the dose-limiting organ in internal and external radiotherapy. As splenectomy is not life threatening, the liver and red marrow were regarded as dose-limiting critical organs for nanoliposome-targeted therapeutics. In external beam therapy, the tolerance dose in the liver is 25 Gy, defined as the dose for a probability of 5% complication in 5 years (TD 5/5) [26]. Due to a lack of dose tolerance in the liver in internal radionuclide therapy, the 25-Gy value was applied to estimate the MAA in a previous study. The tolerance dose in the red marrow of 1.85 Gy was chosen, representing a probability of major platelet toxicity of approximately 30% [27].

Maximum tolerated dose (MTD) of ^{188}Re-cetuximab in normal nude mice

The maximum tolerated dose (MTD) is defined as the highest dose that can be given while still resulting in zero lethality and < 20% body weight loss [28, 29]. The radiation toxicity of ^{188}Re-cetuximab was monitored by an MTD study. Male nude mice were randomly grouped into cages of five and used at age of 8 weeks. Mice were given 22.2, 29.6, 37, 44.4, 51.8 and 59.2 MBq of ^{188}Re-cetuximab (containing cetuximab 37.8 μg per mouse) by single intravenous injection. The mice were weighed twice per week, and the survival rate of the mice was recorded every day. The drug-induced radiation toxicities (lethality and body weight loss) were determined for a minimum of 4 weeks.

Therapeutic efficacy

Twenty-five male nude mice were used and each was subcutaneously inoculated with NCI-H292 cells (2×10^6) in the right hind leg. Treatments were initiated when the volume of tumors became about 50 mm^3. Mice were randomly divided into five groups and one group was randomly selected as the control, with five mice per group (19.8 g on average). Five groups of mice were treated with ^{188}Re-cetuximab (29.6 MBq of ^{188}Re and 37.8 μg/mouse cetuximab), ^{188}Re-cetuximab (22.2 MBq of ^{188}Re and 37.8 μg/mouse cetuximab), ^{188}Re (29.6 MBq of ^{188}Re), cetuximab (37.8 μg/mouse) and normal saline by single i.v. injection, respectively. Tumor was measured twice weekly by a digital caliper to document tumor growth and the survival rate of the mice was recorded. Tumor measurements were converted into tumor volume (V) using the formula $V = (Y \times W^2)/2$; where Y and W are larger and smaller perpendicular diameters, respectively. All data were expressed as mean ± SD. The mean tumor growth inhibition rate (MGI) was calculated according to the volume of the tumor: growth rate of the treated group/growth rate of the untreated group [30]. The combination index (CI) was calculated by dividing the expected growth inhibition rate by the observed growth inhibition rate. An index >1 indicates a synergistic effect [30]. Following standard animal research protocols, termination was mandated on reaching one or both of the following criteria: a tumor weight > 2 g (2 mL volume) or total body weight loss >20% [31].

Statistics

Data were expressed as mean ± SD. The SPSS 11 program (SPSS Inc., USA) was used to perform statistical analysis, and the survival data were estimated by the Kaplan-Meier method and compared by log-rank test. Values of $P < 0.05$ were considered significant.

Results

Labeling efficiency and immunoreactivity

The radiolabeling efficiency and radiochemical purity of ^{188}Re-cetuximab was checked by instant thin layer chromatography and size exclusion-HPLC analysis. The labeling efficiency of ^{188}Re-cetuximab was higher than 95%. The radiochemical purity of ^{188}Re-cetuximab was higher than 95%. The immunoreactivity of ^{188}Re-cetuximab was higher than 75%. These results suggested labeling of radionuclides to cetuximab preserved the binding ability of the antibody. The mole ratio of antibody to ^{188}Re was 27.29.

Pharmacokinetics

The pharmacokinetic parameters were estimated with the WinNonlin program and are summarized in Tables 1 and 2. The maximum concentration (C_{max}) of ^{188}Re-cetuximab at 0.5 h in blood was 23.82 %ID/g. The clearance rate (Cl) of ^{188}Re-cetuximab was 0.17 ml/h. The area under the time curve ($AUC0 \rightarrow_\infty$) of ^{188}Re-cetuximab was 630.49 %ID/g*h. The $T_{1/2z}$ (elimination half-life) of ^{188}Re-cetuximab in blood was 33.19 h.

Table 1 Biodistribution of ^{188}Re-cetuximab in human NCI-H292 lung tumor-bearing nude mice at 4, 24, 48 and 72 h after i.v. injection ($n = 5$). Tumor size was 40–80 mm^3

(%ID/g)	4 h	24 h	48 h	72 h
Whole blood	14.92 ± 1.73	2.57 ± 0.13	1.52 ± 0.13	1.15 ± 0.07
Skin	1.97 ± 0.17	0.98 ± 0.02	0.66 ± 0.06	0.51 ± 0.02
Heart	3.46 ± 0.29	0.57 ± 0.02	0.35 ± 0.02	0.23 ± 0.02
Lung	5.52 ± 1.13	1.34 ± 0.27	1.43 ± 0.59	0.69 ± 0.07
Liver	10.47 ± 1.70	2.43 ± 0.10	1.80 ± 0.12	1.38 ± 0.11
Kidney	8.00 ± 0.42	2.89 ± 0.09	1.82 ± 0.12	1.29 ± 0.09
Spleen	3.48 ± 0.65	0.95 ± 0.07	0.81 ± 0.08	0.72 ± 0.10
Pancreas	1.14 ± 0.10	0.25 ± 0.01	0.16 ± 0.02	0.11 ± 0.01
Stomach	1.65 ± 0.22	0.40 ± 0.02	0.27 ± 0.02	0.18 ± 0.01
Large intestine	1.07 ± 0.09	0.30 ± 0.01	0.20 ± 0.02	0.17 ± 0.01
Small intestine	2.18 ± 0.36	0.47 ± 0.04	0.36 ± 0.04	0.29 ± 0.03
Bone	1.16 ± 0.31	0.31 ± 0.06	0.19 ± 0.03	0.17 ± 0.05
Muscle	0.52 ± 0.08	0.25 ± 0.02	0.17 ± 0.01	0.13 ± 0.03
Tumor	17.58 ± 1.30	25.30 ± 3.15	25.14 ± 1.04	24.79 ± 0.78
Tumor/muscle	45.94 ± 10.71	104.49 ± 12.58	147.89 ± 12.29	230.31 ± 42.98
Tumor/blood	1.24 ± 0.38	9.98 ± 3.31	17.25 ± 5.05	21.94 ± 3.40
Tumor/liver	1.88 ± 0.74	10.32 ± 2.24	14.43 ± 3.73	18.26 ± 2.52

Data were expressed as percentage of injected dose per gram (%ID/g ± standard error, n = 5 at each time-point)

Biodistribution and SPECT/CT imaging of ^{188}Re-cetuximab

Biodistribution of ^{188}Re-cetuximab at 4, 24, 48 and 72 h after intravenous injection is listed in Table 1. The results of ^{188}Re-cetuximab showed significant accumulation in the tumor, liver, spleen and kidney. The fast blood clearance, and rapid excretion from the liver, kidney and spleen were observed. The highest uptake of ^{188}Re-cetuximab in the liver, kidney and spleen reached 10.47% ± 1.70%, 8.00% ± 0.42% and 3.48% ± 0.65% at 4 h after administration, respectively. Very low levels of ^{188}Re-cetuximab uptake were observed in the musculoskeletal systems and other organs. The levels of radioactivity within the tumor peaked at 24 h (25.30% ± 3.15%) and then slowly declined. The tumor uptake of ^{188}Re-cetuximab was steadily maintained until 72 h after administration (24.79% ± 0.78%). The highest Tumor/Muscle (T/M) ratio of ^{188}Re-cetuximab reached 230.31 ± 42.98 at 72 h after injection. The T/M ratios were 45.94 ± 10.71, 104.49 ± 12.58 and 147.89 ± 12.29 at 4, 24 and 48 h, respectively. The highest Tumor/Blood (T/B) ratio of ^{188}Re-cetuximab was reached 21.94 ± 1.52 at 72 h after injection. The T/B ratios were 2.12 ± 0.55, 9.98 ± 1.48 and 17.25 ± 2.26 at 4, 24 and 48 h, respectively.

The longitudinal nanoSPECT/CT imaging of ^{188}Re-cetuximab indicated significant uptake in the tumors at 4 and 24 h after intravenous injection (Figs 1 and 2). The accumulated activity of ^{188}Re-cetuximab in the tumor at time points was calculated from the images created by drawing the region of interest (ROI) using the standard source as a point of reference. The image quantitative analysis of ^{188}Re-cetuximab in the tumor at 1, 4 and 24 h after injection was 2.94 ± 0.38, 7.32 ± 1.19 and 10.23 ± 0.77 %ID/g, respectively. The trend of uptake analyzed by imaging is similar to the results of biodistribution (Table 1).

Table2 Pharmarcokinetic parameters of ^{188}Re-cetuximab after intravenous injection in normal nude mice ($n = 8$)

Parameters	
C_{max} (%ID/mL)	23.82
Cl (mL/h)	0.17
$AUC_{0\rightarrow\infty}$(%ID /mL*h)	630.49
$T_{1/2Z}$ (h)	27.12
$MRT_{0\rightarrow\infty}$ (h)	33.19

Pharmacokinetic parameters were determined using the WinNonlin software version 5.3 (Pharsight Corp., Mountain View, CA)

C_{max} maximum concentration, *Cl* clearance rate, *AUC* area under curve, *$T_{1/2Z}$* elimination half-life, *MRT* mean residence time

Dosimetry of ^{188}Re-cetuximab

According to the mouse biodistribution results (Table 1), the radiation-absorbed doses for administering intravenously ^{188}Re-cetuximab in major human organs were estimated by the OLINDA program, as shown in Table 3. The radiation doses absorbed by the liver, kidney, spleen and total body

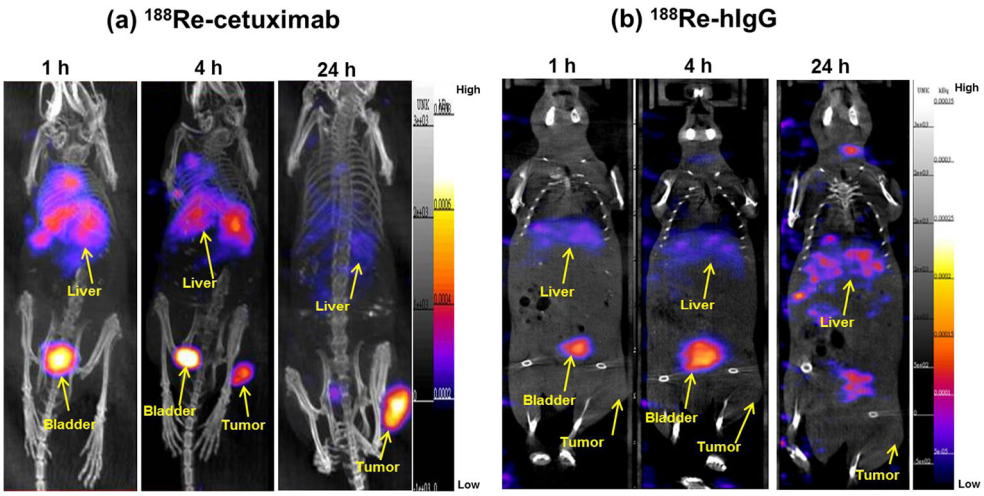

Fig. 1 Comparisons of nanoSPECT/CT images of ^{188}Re-cetuximab (**a**) or ^{188}Re-human IgG (**b**) targeting NCI-H292 tumors bearing in nude mice (100~150 mm^3). The ^{188}Re-cetuximab and ^{188}Re-human IgG containing 12.95 MBq of ^{188}Re was administered to each mouse by intravenous injection ($n = 3$). The images were acquired at 1, 4, and 24 h after injection. The result indicates ^{188}Re-cetuximab is a potential theranostic agent for EGFR-positive tumors

were 0.167, 0.143, 0.0591 and 0.0559 mGy/MBq, respectively. To estimate the recommended MAA of the ^{188}Re-cetuximab, the tolerance dose delivered in critical organs, liver, and red marrow, should be lower than the tolerance doses of both liver and red marrow following the injection of the MAA. If the liver was initially regarded as the critical organ, the MAA of ^{188}Re-cetuximabe was 149.7 GBq. However, the red marrow–absorbed dose delivered from such an administration would be higher than levels generally associated with dose-limiting toxicity in red marrow (1.85 Gy). If red marrow was regarded as the critical organ, the MAA of ^{188}Re-cetuximabe was 33 GBq (Table 4). The liver-absorbed dose delivered from such an administration was 5.52 Gy, which is lower than the levels generally associated with dose-limiting toxicity in the liver (25 Gy).

Maximum tolerated dose (MTD)

To identify the radiation MTDs of ^{188}Re-cetuximab, mice without NCI-H292 tumor were treated with various therapeutics doses (22.2, 29.6, 37, 44.4, 51.8 and 59.2 MBq). There was no significant decrease in body weight and drug-induced death of normal BALB/c mice administered 22.2, 29.6 and 37 MBq of cetuximab by single i.v. injection. Except for the control group, all groups of mice were at the lowest body weight on day 7 after the injection, and gradually recovered. The decrease in body weight was dose-dependent in mice with ^{188}Re-cetuximab. For MTD, the maximum dose with weight loss less than 20% of ^{188}Re-cetuximab was determined to be 37 MBq.

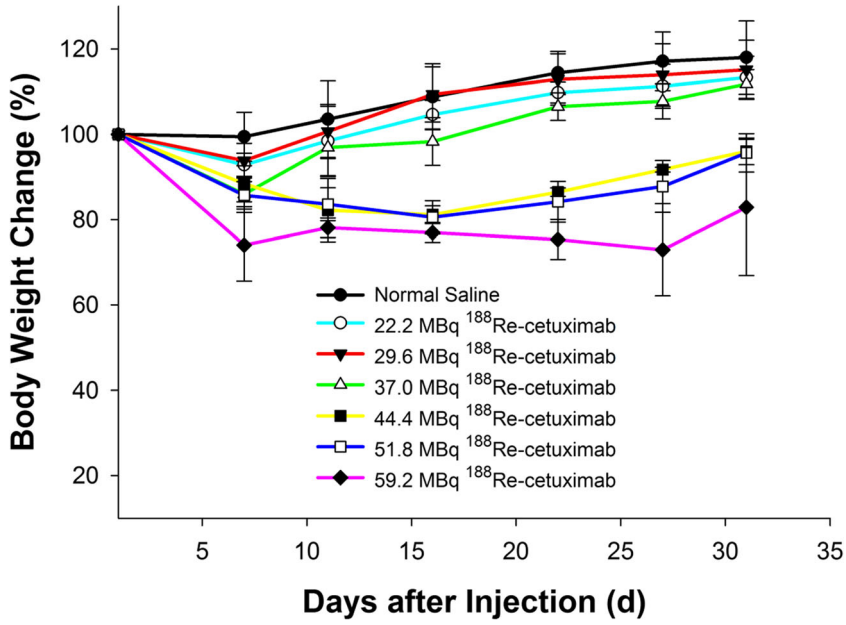

Fig. 2 MTD determination of ^{188}Re-cetuximab in normal nude mice by single i.v. injection. Six doses at 7.4 MBq intervals were evaluated. The MTD is defined as the highest dose that can be given while still resulting in zero lethality and < 20% body weight loss

Table 3 Absorbed doses (mGy/MBq) of ^{188}Re-cetuximab in NCI-H292 lung tumor-bearing nude mice by single injection

Normal organs	Absorbed doses (mGy/MBq)
Brain	0.079
Heart wall	0.160
Kidneys	0.143
Liver	0.167
Lungs	0.147
Spleen	0.059
Testes	0.079
Effective dose	0.088
Total body	0.092

Therapeutic efficacy

The tumor volume growth and inhibition following various treatments from 0 to 29 days were plotted in Fig. 3. As shown in Fig. 3, a time-dependent increase in tumor volume was observed in the normal saline control and cetuximab-treated groups. In contrast to the mean tumor volume of 1291.1 ± 457.8 mm^3 in the untreated normal saline group at 29 d, the mean tumor volume of the treated groups at 29 d with a single dose administration of cetuximab (37.8 μg per mouse), free ^{188}Re (29.6 MBq), 22.2 MBq ^{188}Re-cetuximab (containing 37.8 μg cetuximab per mouse) and 29.6 MBq ^{188}Re-cetuximab (containing 37.8 μg cetuximab per mouse) were 939.6 ± 441.2 mm^3, 937.5 ± 537.2 mm^3, 96.1 ± 57.0 mm^3 and 63.2 ± 40.3 mm^3, respectively. As shown in Fig. 3, the mean growth inhibition rates achieved by cetuximab, 29.6 MBq free ^{188}Re, 22.2 MBq ^{188}Re-cetuximab and 29.6 MBq ^{188}Re-cetuximab were 0.708, 0.642, 0.049 and 0.074, respectively. An extremely significant synergistic tumor growth inhibition effect was demonstrated by the radiochemo-combination treatment with 22.2 MBq ^{188}Re-cetuximab and 29.6 MBq ^{188}Re-cetuximab (CI = 9.276 and 6.135; Table 5).

Table 4 Maximum administered activity estimated from animal studies for a 70-kg male model at red marrow was regarded as the critical organ

		Absorbed dose			
Red marrow (mGy/MBq)	Estimated ID (mCi, GBq)	Liver (Gy)	Kidney (Gy)	Spleen (Gy)	Tumor (Gy)
0.0559	894, 33	5.52	4.73	1.95	327

MTD is 25 Gy for liver, considered as a critical organ and is 1.85 Gy for red marrow. MAA of tumor was calculated as 300 g

The survival curves for the different treatment groups are compared in Fig. 4. The median survival time for the normal saline control mice was 36.75 d. The median survival times for the mice treated with cetuximab (37.8 μg cetuximab per mouse), 29.6 MBq free ^{188}Re, 22.2 MBq ^{188}Re-cetuximab and 29.6 MBq ^{188}Re-cetuximab were 62.75, 42.25, 62.50 ($P < 0.05$) and 61.75 d ($P < 0.05$), respectively. The P values for the differences among the survival curves of the various treatment groups are shown in Table 5. At the end of the experiment (66 days after therapeutic administration), one mice (20%) treated with 22.2 MBq ^{188}Re-cetuximab and 29.6 MBq ^{188}Re-cetuximab survived.

The group treated with cetuximab (37.8 μg cetuximab per mouse), 29.6 MBq free ^{188}Re, 22.2 MBq ^{188}Re-cetuximab and 29.6 MBq ^{188}Re-cetuximab displayed a slight loss in body weight (Fig. 5). The reduction in body weight for mice treated with cetuximab (37.8 μg/mouse), 29.6 MBq free ^{188}Re, 22.2 MBq ^{188}Re-cetuximab and 29.6 MBq ^{188}Re-cetuximab were no more than 10%.

Discussion

Targeting EGFR based on its specific antibody is useful and has potential for developing a diagnostic methodology for EGFR-positive tumors. Utilization of radiolabeled cetuximab has been applied for diagnosing tumors such as colorectal cancer (CRC) [32] or head and neck tumor [33]. Currently, cetuximab has been labeled with ^{111}In [34–36], ^{89}Zr [37, 38], ^{64}Cu [39, 40], ^{99m}Tc [41], ^{90}Y and ^{177}Lu [42, 43]. which is insufficient to in antibody-based nuclear imaging such as cetuximab with the apparent imaging signals after 4 to 72 h injection. ^{89}Zr and ^{64}Cu are PET isotopes having higher resolution than SPECT imaging such as images derived from ^{177}Lu and ^{111}In. ^{64}Cu has potential applications in diagnostic imaging and radiotherapy due to the additional β^- particles emitting. The characteristics of ^{188}Re for its use in palliative or radiotherapy come from a short physical half-life of 16.9 h with a high energy tissue penetration range of 2.12 MeV and LET 0.2 kev/μm of β^- particles. Its 155 keV (15%) γ-rays are quite suitable for nuclear imaging. The high-energy beta emitters of ^{188}Re (2.12 MeV) have a mean tissue penetration range of 3.5 mm and maximum tissue penetration range of 10.15 mm [44, 45], enabling ^{188}Re to kill tumor cells through a cross-fire or nonspecific cell-killing effect. Among various available radioisotopes, we have chosen ^{188}Re for radiolabelling with cetuximab because synergistic utilization of these radioisotopes could potentially lead to the development of a personalized approach for radioimmunotherapy (RIT).

In this study, ^{188}Re-cetuximab was demonstrated to diagnose an early small tumor (Table 1) and advanced large tumor (Fig. 1). The biodistribution pattern and tumor uptake for ^{111}In-cetuximab [36], ^{90}Y-CHX-A-DTPA-cetuximab and

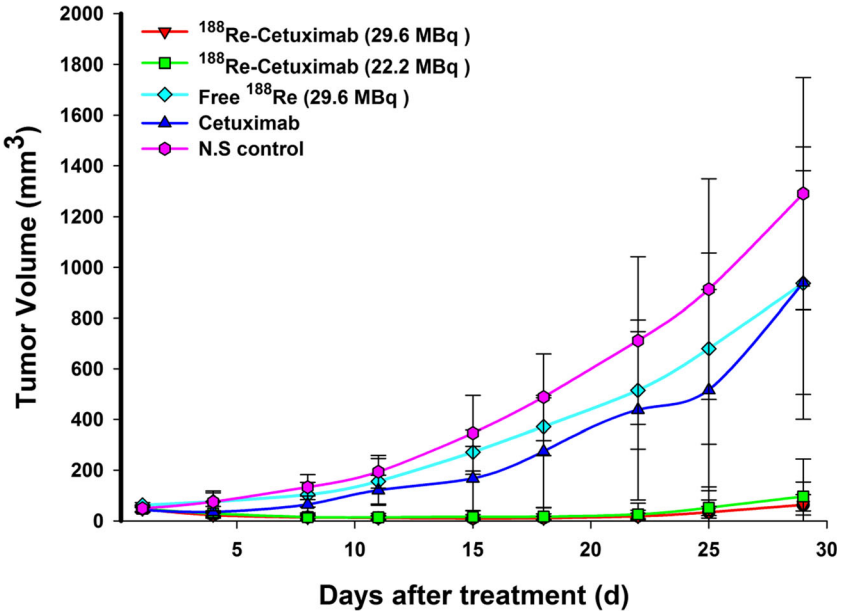

Fig. 3 Tumor growth curves. Tumor growth volume (mm^3) versus time (days) for nude mice implanted with NCI-H292 human lung tumors after administering ^{188}Re-cetuximab (29.6 and 22.2 MBq), free ^{188}Re (29.6 MBq), cetuximab (37.8 μg/mouse) and normal saline by single i.v. injection

^{177}Lu-CHX-A-DTPA-cetuximab [42] were compared with ^{188}Re-cetuximab. The tumor uptake of ^{188}Re-cetuximab was measured to be 25.3 %ID/g, which was higher than that of ^{90}Y-CHX-A-DTPA-cetuximab (15.9 %ID/g) and ^{177}Lu-CHX-A-DTPA-cetuximab (17.6 %ID/g) at 24 h after injection. The tumor to muscle ratio of ^{188}Re-cetuximab was measured 104-fold, which was higher than that of ^{111}In-cetuximab, ^{90}Y-CHX-A-DTPA-cetuximab and ^{177}Lu-CHX-A-DTPA-cetuximab measured as 7.5-fold, ~30-fold and ~40-fold at 24 h after injection, respectively. The high liver observed in case of radiolabelled mAbs is not unexpected because these macromolecules (~150 kDa molecular weight) mainly clear from the biological system through the hepatic route. Moreover, it is well known the liver displays relatively high levels of EGFR leading to increased uptake of radiolabelled cetuximab in the liver. The liver uptake of ^{188}Re-cetuximab increases rapidly at 4 h (10.47 ± 1.70 %ID/g) and reduce quickly at 72 h (1.38 ± 0.11 %ID/g). The tumor-to-liver ratio was observed to increase from 1.88 ± 0.74 at 4 h to 18.26 ± 2.52 at 72 h. For ^{177}Lu-CHX-A-DTPA-cetuximab, the tumor-to-liver ratio was observed to increase from 0.46 ± 0.21 at 4 h to 2.83 ± 0.98 at 72 h. For ^{90}Y-CHX-A-DTPA-cetuximab, the tumor-to-liver ratio was observed to increase from 0.37 ± 0.16 at 4 h to 2.67 ± 0.44 at 72 h.

Table 5 Therapeutic efficacy of ^{188}Re-cetuximab on NCI-H292 lung tumor-bearing nude mice by single injection

Treatment modality	Tumor growth inhibition			Survival		
	MGI[a]	Expected[b]	CI[c]	median survival time (d)	*P* value[d]	lifespan[e] (%)
^{188}Re-cetucimab (22.2 MBq)	0.049	0.454	9.276	62.50	0.002	70.07
^{188}Re-cetucimab (29.6 MBq)	0.074	0.454	6.135	61.75	0.002	68.03
Cetuximab (37.8 μg/mouse)	0.708	–	–	42.75	0.047	16.33
Free ^{188}Re (29.6 MBq)	0.642	–	–	42.25	0.167	14.97
Normal Saline Control	–	–	–	36.75	–	–

[a] MGI, Mean growth inhibition rate = Growth rate of treated group/Growth rate of untreated group. (at 29 days after administration)

[b] Expected growth inhibition rate = Growth inhibition rate of free ^{188} Re x Growth inhibition rate of cetuximab

[c] CI, combination index was calculated by dividing the expected growth inhibition rate by the observed growth inhibition rate. An index > 1 indicates synergistic effect [30]

[d] *P* values were estimated between the experimental and normal saline control groups by log-rank test, $P < 0.05$ indicates significance

[e] Percentage increase in lifespan was expressed as (T/C - 1) × 100%, where T is the median survival time of treated mice and C is the median survival time of control mice

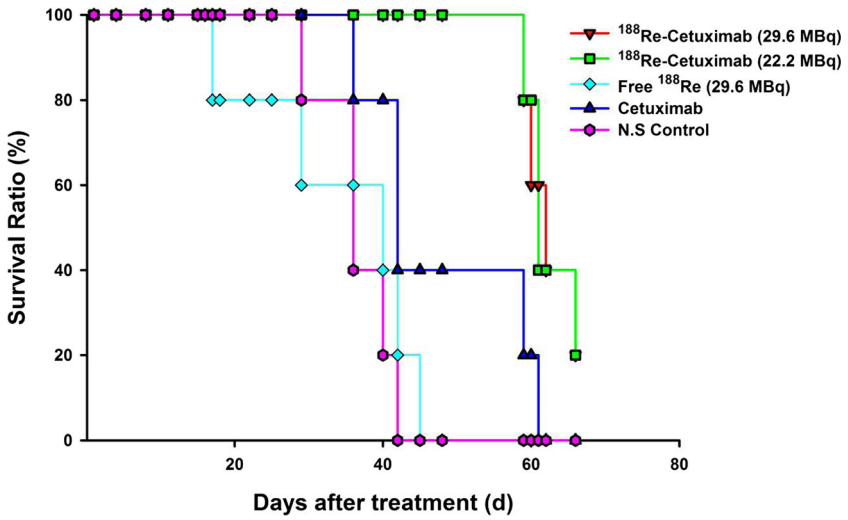

Fig. 4 Survival curves for nude mice implanted with NCI-H292 human lung tumors after administering ^{188}Re-cetuximab (29.6 and 22.2 MBq), free ^{188}Re (29.6 MBq), cetuximab (37.8 μg/mouse) and normal saline by single i.v. injection

Rhenium-188 emits a gamma photon (155-keV) and a beta particle (2.12 MeV) suitable for nuclear imaging and radiotherapy. Comparing the physical properties of radionuclides, the maximum beta energy of ^{188}Re (2.12 MeV) is better than ^{177}Lu (0.497 MeV) and similar to ^{90}Y (2.84 MeV). The high-energy beta emitters of ^{188}Re have a mean tissue penetration range of 3.5 mm and maximum tissue penetration range of 10.15 mm. [44, 45], enabling ^{188}Re to kill tumor cells through a cross-fire or nonspecific cell-killing effect. Wang et al. [46] studied therapies of Re-188-labeled herceptin, finding the tumor growth of the DU145 xenografts in SCID mice was inhibited exclusively by Re-188-labeled Herceptin treatment; the tumor growth inhibition (TGI) calculated as the ratio of tumor volume (treatments/control) at day 55 was 36.6%. Li et al. [47] studied the therapeutic efficacy of radioimmunotherapy of ^{188}Re-labeled herceptin; the tumor inhibition rate (IR) was 48.8 ± 4.9 after the fourth week of ^{188}Re-herceptin (11.1 MBq) administration by intravenous injection. In this investigation, the results (Table 5) of comparisons of therapeutic treatment with ^{188}Re-cetuximab and cetuximab revealed ^{188}Re-cetuximab showed a better tumor growth inhibition rate and a higher survival ratio and lifespan of NCI-H292 tumor-bearing mice treated with single doses (0.049, 62.5 days and 70.07%, respectively).

reclinical data indicate the anti-epidermal growth factor receptor (EGFR) agent cetuximab (Erbitux) as a radiosensitizer. EGFR-mediated radioresistance has been

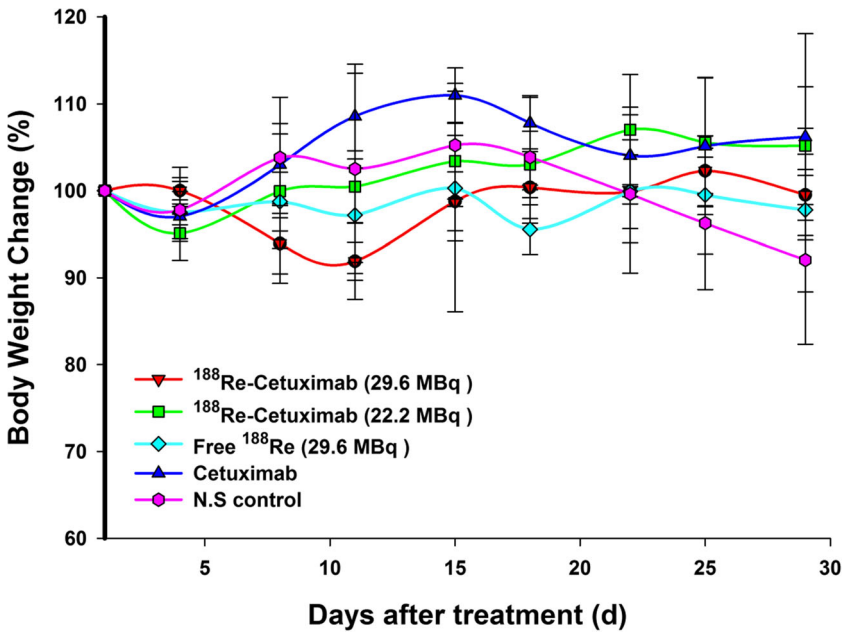

Fig. 5 Body weight change for nude mice implanted with NCI-H292 human lung tumors after administering ^{188}Re-cetuximab (29.6 and 22.2 MBq), free ^{188}Re (29.6 MBq), cetuximab (37.8 μg/mouse) and normal saline by single i.v. injection

evidenced by EGFR activation and stimulation of DNA repair by ionizing radiation [48, 49], and the ability of anti-EGFR agents to enhance radiation in pancreatic cancer has been demonstrated in animal studies [50, 51]. The inhibition of EGFR has resulted in clinically significant radiosensitization for locoregionally advanced tumors [14, 21, 52, 53]. In this study, synergistic effect of ^{188}Re-cetuximab was demonstrated. The synergistic effect may be caused by radiosensitization of cetuximab. For this speculation, further research is needed.

Conclusion

The tumor targeting and localization of ^{188}Re-cetuximab were confirmed by the biodistribution, pharmacokinetics and in vivo nanoSPECT/CT imaging. The therapeutic efficacy of the ^{188}Re-cetuximab was proven in NCI-H292 lung carcinoma tumor-bearing nude mice. The synergistic therapeutic efficacy was demonstrated for the radioimmunotherapy of ^{188}Re-cetuximab. The results of SPECT/CT imaging and therapeutic efficacy study reveal the potential advantage and benefit obtained from ^{188}Re-cetuximab for oncology diagnosis and therapy applications in the future.

Acknowledgements The authors would like to thank C. C. Liang, W. L. Lo, Y. R. Huang and M. W. Chen for help with the biodistribution study of ^{188}Re-cetuximab.

Grants This study was supported by the grants from Ministry of Economic Affairs of Taiwan (Grant Number 107-EC-17-A-22-1309) and Taipei Veterans General Hospital (Grant Number V106D29–003-MY3–2).

Compliance with ethical standards

Conflict of interest All authors have no conflict of interest.

Ethical approval This article does not contain any studies with human participants performed by any of the authors.

Publisher's Note Springer Nature remains neutral with regard to jurisdictional claims in published maps and institutional affiliations.

References

1. Molina JR, Yang P, Cassivi SD, Schild SE, Adjei AA (2008) Non-small cell lung cancer: epidemiology, risk factors, treatment, and survivorship. Mayo Clin Proc 83(5):584–594. https://doi.org/10.4065/83.5.584
2. Privitera G, Luca T, Musso N, Vancheri C, Crimi N, Barresi V, Condorelli D, Castorina S (2016) In vitro antiproliferative effect of trastuzumab (Herceptin((R))) combined with cetuximab (Erbitux((R))) in a model of human non-small cell lung cancer expressing EGFR and HER2. Clin Exp Med 16(2):161–168. https://doi.org/10.1007/s10238-015-0343-8
3. Patil N, Abba M, Allgayer H (2012) Cetuximab and biomarkers in non-small-cell lung carcinoma. Biologics 6:221–231. https://doi.org/10.2147/BTT.S24217
4. Pujol JL, Pirker R, Lynch TJ, Butts CA, Rosell R, Shepherd FA, Vansteenkiste J, O'Byrne KJ, de Blas B, Heighway J, von Heydebreck A, Thatcher N (2014) Meta-analysis of individual patient data from randomized trials of chemotherapy plus cetuximab as first-line treatment for advanced non-small cell lung cancer. Lung Cancer 83(2):211–218. https://doi.org/10.1016/j.lungcan.2013.11.006
5. Kim SM, Kim JS, Kim JH, Yun CO, Kim EM, Kim HK, Solca F, Choi SY, Cho BC (2010) Acquired resistance to cetuximab is mediated by increased PTEN instability and leads cross-resistance to gefitinib in HCC827 NSCLC cells. Cancer Lett 296(2):150–159. https://doi.org/10.1016/j.canlet.2010.04.006
6. Pirker R, Pereira JR, Szczesna A, von Pawel J, Krzakowski M, Ramlau R, Vynnychenko I, Park K, Yu CT, Ganul V, Roh JK, Bajetta E, O'Byrne K, de Marinis F, Eberhardt W, Goddemeier T, Emig M, Gatzemeier U, Team FS (2009) Cetuximab plus chemotherapy in patients with advanced non-small-cell lung cancer (FLEX): an open-label randomised phase III trial. Lancet 373(9674):1525–1531. https://doi.org/10.1016/S0140-6736(09)60569-9
7. Rosell R, Robinet G, Szczesna A, Ramlau R, Constenla M, Mennecier BC, Pfeifer W, O'Byrne KJ, Welte T, Kolb R, Pirker R, Chemaissani A, Perol M, Ranson MR, Ellis PA, Pilz K, Reck M (2008) Randomized phase II study of cetuximab plus cisplatin/vinorelbine compared with cisplatin/vinorelbine alone as first-line therapy in EGFR-expressing advanced non-small-cell lung cancer. Annals of oncology : official journal of the European Society for. Med Oncol 19(2):362–369. https://doi.org/10.1093/annonc/mdm474
8. Gatzemeier U, von Pawel J, Vynnychenko I, Zatloukal P, de Marinis F, Eberhardt WE, Paz-Ares L, Schumacher KM, Goddemeier T, O'Byrne KJ, Pirker R (2011) First-cycle rash and survival in patients with advanced non-small-cell lung cancer receiving cetuximab in combination with first-line chemotherapy: a subgroup analysis of data from the FLEX phase 3 study. Lancet Oncol 12(1):30–37. https://doi.org/10.1016/S1470-2045(10)70278-3
9. Milenic DE, Brady ED, Brechbiel MW (2004) Antibody-targeted radiation cancer therapy. Nat Rev Drug Discov 3(6):488–499. https://doi.org/10.1038/nrd1413
10. Ting G, Chang CH, Wang HE, Lee TW (2010) Nanotargeted radionuclides for cancer nuclear imaging and internal radiotherapy. J Biomed Biotechnol 2010:1–17. https://doi.org/10.1155/2010/953537
11. Davis TA, Kaminski MS, Leonard JP, Hsu FJ, Wilkinson M, Zelenetz A, Wahl RL, Kroll S, Coleman M, Goris M, Levy R, Knox SJ (2004) The radioisotope contributes significantly to the activity of radioimmunotherapy. Clin Cancer Res 10(23):7792–7798. https://doi.org/10.1158/1078-0432.CCR-04-0756
12. Witzig TE, Gordon LI, Cabanillas F, Czuczman MS, Emmanouilides C, Joyce R, Pohlman BL, Bartlett NL, Wiseman GA, Padre N, Grillo-Lopez AJ, Multani P, White CA (2002) Randomized controlled trial of yttrium-90-labeled ibritumomab tiuxetan radioimmunotherapy versus rituximab immunotherapy for patients with relapsed or refractory low-grade, follicular, or transformed B-cell non-Hodgkin's lymphoma. J Clin Oncol 20(10):2453–2463. https://doi.org/10.1200/JCO.2002.11.076
13. Gordon LI, Witzig T, Molina A, Czuczman M, Emmanouilides C, Joyce R, Vo K, Theuer C, Pohlman B, Bartlett N, Wiseman G, Darif M, White C (2004) Yttrium 90-labeled ibritumomab tiuxetan radioimmunotherapy produces high response rates and durable remissions in patients with previously treated B-cell lymphoma. Clin Lymphoma 5(2):98–101
14. Bonner JA (2016) Cetuximab or cisplatin as a radiosensitizer in locoregionally advanced head and neck cancer: recent results.

Transl Cancer Res 5(3):234–237. https://doi.org/10.21037/tcr.2016.06.22
15. Bianco C, Tortora G, Bianco R, Caputo R, Veneziani BM, Caputo R, Damiano V, Troiani T, Fontanini G, Raben D, Pepe S, Bianco AR, Ciardiello F (2002) Enhancement of antitumor activity of ionizing radiation by combined treatment with the selective epidermal growth factor receptor-tyrosine kinase inhibitor ZD1839 (Iressa). Clin Cancer Res 8(10):3250–3258
16. Chinnaiyan P, Huang S, Vallabhaneni G, Armstrong E, Varambally S, Tomlins SA, Chinnaiyan AM, Harari PM (2005) Mechanisms of enhanced radiation response following epidermal growth factor receptor signaling inhibition by erlotinib (Tarceva). Cancer Res 65(8):3328–3335. https://doi.org/10.1158/0008-5472.CAN-04-3547
17. Raben D, Helfrich B, Chan DC, Ciardiello F, Zhao L, Franklin W, Baron AE, Zeng C, Johnson TK, Bunn PA Jr (2005) The effects of cetuximab alone and in combination with radiation and/or chemotherapy in lung cancer. Clin Cancer Res 11(2 Pt 1):795–805
18. Milas L, Mason K, Hunter N, Petersen S, Yamakawa M, Ang K, Mendelsohn J, Fan Z (2000) In vivo enhancement of tumor radioresponse by C225 antiepidermal growth factor receptor antibody. Clin Cancer Res 6(2):701–708
19. Huang SM, Bock JM, Harari PM (1999) Epidermal growth factor receptor blockade with C225 modulates proliferation, apoptosis, and radiosensitivity in squamous cell carcinomas of the head and neck. Cancer Res 59(8):1935–1940
20. Bonner JA, Harari PM, Giralt J, Azarnia N, Shin DM, Cohen RB, Jones CU, Sur R, Raben D, Jassem J, Ove R, Kies MS, Baselga J, Youssoufian H, Amellal N, Rowinsky EK, Ang KK (2006) Radiotherapy plus cetuximab for squamous-cell carcinoma of the head and neck. N Engl J Med 354(6):567–578. https://doi.org/10.1056/NEJMoa053422
21. Bonner JA, Harari PM, Giralt J, Cohen RB, Jones CU, Sur RK, Raben D, Baselga J, Spencer SA, Zhu J, Youssoufian H, Rowinsky EK, Ang KK (2010) Radiotherapy plus cetuximab for locoregionally advanced head and neck cancer: 5-year survival data from a phase 3 randomised trial, and relation between cetuximab-induced rash and survival. Lancet Oncol 11(1):21–28. https://doi.org/10.1016/S1470-2045(09)70311-0
22. Stabin MG, Siegel JA (2003) Physical models and dose factors for use in internal dose assessment. Health Phys 85(3):294–310
23. Molina-Trinidad EM, de Murphy CA, Ferro-Flores G, Murphy-Stack E, Jung-Cook H (2006) Radiopharmacokinetic and dosimetric parameters of ^{188}Re-lanreotide in athymic mice with induced human cancer tumors. Int J Pharm 310(1–2):125–130. https://doi.org/10.1016/j.ijpharm.2005.11.043
24. Lin YY, Chang CH, Li JJ, Stabin MG, Chang YJ, Chen LC, Lin MH, Tseng YL, Lin WJ, Lee TW, Ting G, Chang CA, Chen FD, Wang HE (2011) Pharmacokinetics and dosimetry of ^{111}In/^{188}Re-labeled PEGylated liposomal drugs in two colon carcinoma-bearing mouse models. Cancer Biother Radiopharm 26(3):373–380. https://doi.org/10.1089/cbr.2010.0906
25. Chang CH, Stabin MG, Chang YJ, Chen LC, Chen MH, Chang TJ, Lee TW, Ting G (2008) Comparative dosimetric evaluation of nanotargeted ^{188}Re-(DXR)-liposome for internal radiotherapy. Cancer Biother Radiopharm 23(6):749–758. https://doi.org/10.1089/cbr.2008.0489
26. Bentel GCNC, Noell KT (1989) Treatment planning and dose calculation in radiation oncology. Pergamon Press, Oxford
27. O'Donoghue JA, Baidoo N, Deland D, Welt S, Divgi CR, Sgouros G (2002) Hematologic toxicity in radioimmunotherapy: dose-response relationships for I-131 labeled antibody therapy. Cancer Biother Radiopharm 17(4):435–443
28. Cao S, Rustum YM (2000) Synergistic antitumor activity of irinotecan in combination with 5-fluorouracil in rats bearing advanced colorectal cancer: role of drug sequence and dose. Cancer Res 60(14):3717–3721
29. Reilly RM, Chen P, Wang J, Scollard D, Cameron R, Vallis KA (2006) Preclinical pharmacokinetic, biodistribution, toxicology, and dosimetry studies of ^{111}In-DTPA-human epidermal growth factor: an auger electron-emitting radiotherapeutic agent for epidermal growth factor receptor-positive breast cancer. J Nucl Med 47(6):1023–1031
30. Morgillo F, Kim WY, Kim ES, Ciardiello F, Hong WK, Lee HY (2007) Implication of the insulin-like growth factor-IR pathway in the resistance of non-small cell lung cancer cells to treatment with gefitinib. Clin Cancer Res 13(9):2795–2803. https://doi.org/10.1158/1078-0432.CCR-06-2077
31. Maddalena ME, Fox J, Chen J, Feng W, Cagnolini A, Linder KE, Tweedle MF, Nunn AD, Lantry LE (2009) ^{177}Lu-AMBA biodistribution, radiotherapeutic efficacy, imaging, and autoradiography in prostate cancer models with low GRP-R expression. J Nucl Med 50(12):2017–2024
32. Goetz M, Hoetker MS, Diken M, Galle PR, Kiesslich R (2013) In vivo molecular imaging with cetuximab, an anti-EGFR antibody, for prediction of response in xenograft models of human colorectal cancer. Endoscopy 45(6):469–477. https://doi.org/10.1055/s-0032-1326361
33. van Dijk LK, Hoeben BA, Kaanders JH, Franssen GM, Boerman OC, Bussink J (2013) Imaging of epidermal growth factor receptor expression in head and neck cancer with SPECT/CT and ^{111}In-labeled cetuximab-F(ab')2. J Nucl Med 54(12):2118–2124. https://doi.org/10.2967/jnumed.113.123612
34. Shih YH, Peng CL, Lee SY, Chiang PF, Yao CJ, Lin WJ, Luo TY, Shieh MJ (2015) ^{111}In-cetuximab as a diagnostic agent by accessible epidermal growth factor (EGF) receptor targeting in human metastatic colorectal carcinoma. Oncotarget 6(18):16601–16610. https://doi.org/10.18632/oncotarget.3968
35. Hoeben BA, Molkenboer-Kuenen JD, Oyen WJ, Peeters WJ, Kaanders JH, Bussink J, Boerman OC (2011) Radiolabeled cetuximab: dose optimization for epidermal growth factor receptor imaging in a head-and-neck squamous cell carcinoma model. Int J Cancer 129(4):870–878. https://doi.org/10.1002/ijc.25727
36. Shih BB, Chang YF, Cheng CC, Yang HJ, Chang KW, Ho AS, Lin HC, Yeh C, Chang CC (2017) SPECT imaging evaluation of ^{111}indium-chelated cetuximab for diagnosing EGFR-positive tumor in an HCT-15-induced colorectal xenograft. J Chin Med Assoc 80(12):766–773. https://doi.org/10.1016/j.jcma.2017.02.010
37. Makris NE, Boellaard R, van Lingen A, Lammertsma AA, van Dongen GA, Verheul HM, Menke CW, Huisman MC (2015) PET/CT-derived whole-body and bone marrow dosimetry of ^{89}Zr-cetuximab. J Nucl Med 56(2):249–254. https://doi.org/10.2967/jnumed.114.147819
38. Perk LR, Visser GW, Vosjan MJ, Stigter-van Walsum M, Tijink BM, Leemans CR, van Dongen GA (2005) ^{89}Zr as a PET surrogate radioisotope for scouting biodistribution of the therapeutic radiometals ^{90}Y and ^{177}Lu in tumor-bearing nude mice after coupling to the internalizing antibody cetuximab. J Nucl Med 46(11):1898–1906
39. van Dijk LK, Yim CB, Franssen GM, Kaanders JH, Rajander J, Solin O, Gronroos TJ, Boerman OC, Bussink J (2016) PET of EGFR with ^{64}Cu-cetuximab-F(ab')2 in mice with head and neck squamous cell carcinoma xenografts. Contrast Media Mol Imaging 11(1):65–70. https://doi.org/10.1002/cmmi.1659
40. Guo Y, Parry JJ, Laforest R, Rogers BE, Anderson CJ (2013) The role of p53 in combination radioimmunotherapy with ^{64}Cu-DOTA-cetuximab and cisplatin in a mouse model of colorectal cancer. J Nucl Med 54(9):1621–1629. https://doi.org/10.2967/jnumed.112.118539
41. Schechter NR, Wendt RE 3rd, Yang DJ, Azhdarinia A, Erwin WD, Stachowiak AM, Broemeling LD, Kim EE, Cox JD, Podoloff DA, Ang KK (2004) Radiation dosimetry of ^{99m}Tc-labeled C225 in patients with squamous cell carcinoma of the head and neck. J Nucl Med 45(10):1683–1687

42. Chakravarty R, Chakraborty S, Sarma HD, Nair KV, Rajeswari A, Dash A (2016) $^{90}Y/^{177}Lu$-labelled Cetuximab immunoconjugates: radiochemistry optimization to clinical dose formulation. J Label Compd Radiopharm 59(9):354–363. https://doi.org/10.1002/jlcr.3413
43. Song IH, Lee TS, Park YS, Lee JS, Lee BC, Moon BS, An GI, Lee HW, Kim KI, Lee YJ, Kang JH, Lim SM (2016) Immuno-PET imaging and Radioimmunotherapy of $^{64}Cu-/^{177}Lu$-labeled anti-EGFR antibody in esophageal squamous cell carcinoma model. J Nucl Med 57(7):1105–1111. https://doi.org/10.2967/jnumed.115.167155
44. Iznaga-Escobar N (1998) ^{188}Re-direct labeling of monoclonal antibodies for radioimmunotherapy of solid tumors: biodistribution, normal organ dosimetry, and toxicology. Nucl Med Biol 25(5):441–447
45. O'Donoghue JA, Bardies M, Wheldon TE (1995) Relationships between tumor size and curability for uniformly targeted therapy with beta-emitting radionuclides. Journal of nuclear medicine : official publication, Society of Nuclear Medicine 36(10):1902–1909
46. Wang HY, Lin WY, Chen MC, Lin T, Chao CH, Hsu FN, Lin E, Huang CY, Luo TY, Lin H (2013) Inhibitory effects of Rhenium-188-labeled Herceptin on prostate cancer cell growth: a possible radioimmunotherapy to prostate carcinoma. Int J Radiat Biol 89(5):346–355. https://doi.org/10.3109/09553002.2013.762136
47. Li G, Wang Y, Huang K, Zhang H, Peng W, Zhang C (2005) The experimental study on the radioimmunotherapy of the nasopharyngeal carcinoma overexpressing HER2/neu in nude mice model with intratumoral injection of ^{188}Re-herceptin. Nucl Med Biol 32(1):59–65. https://doi.org/10.1016/j.nucmedbio.2004.09.003
48. Dittmann K, Mayer C, Fehrenbacher B, Schaller M, Raju U, Milas L, Chen DJ, Kehlbach R, Rodemann HP (2005) Radiation-induced epidermal growth factor receptor nuclear import is linked to activation of DNA-dependent protein kinase. J Biol Chem 280(35):31182–31189. https://doi.org/10.1074/jbc.M506591200
49. Dittmann K, Mayer C, Fehrenbacher B, Schaller M, Kehlbach R, Rodemann HP (2011) Nuclear epidermal growth factor receptor modulates cellular radio-sensitivity by regulation of chromatin access. Radiother Oncol 99(3):317–322. https://doi.org/10.1016/j.radonc.2011.06.001
50. Morgan MA, Parsels LA, Kollar LE, Normolle DP, Maybaum J, Lawrence TS (2008) The combination of epidermal growth factor receptor inhibitors with gemcitabine and radiation in pancreatic cancer. Clin Cancer Res 14(16):5142–5149. https://doi.org/10.1158/1078-0432.CCR-07-4072
51. Kimple RJ, Vaseva AV, Cox AD, Baerman KM, Calvo BF, Tepper JE, Shields JM, Sartor CI (2010) Radiosensitization of epidermal growth factor receptor/HER2-positive pancreatic cancer is mediated by inhibition of Akt independent of ras mutational status. Clin Cancer Res 16(3):912–923. https://doi.org/10.1158/1078-0432.CCR-09-1324
52. Rembielak AI, Jain P, Jackson AS, Green MM, Santorelli GR, Whitfield GA, Crellin A, Garcia-Alonso A, Radhakrishna G, Cullen J, Taylor MB, Swindell R, West CM, Valle J, Saleem A, Price PM (2014) Phase II trial of Cetuximab and conformal radiotherapy only in locally advanced pancreatic Cancer with concurrent tissue sampling feasibility study. Transl Oncol 7(1):55–64
53. Bonner JA, Trummell HQ, Bonner AB, Willey CD, Bredel M, Yang ES (2015) Enhancement of Cetuximab-induced Radiosensitization by JAK-1 inhibition. BMC Cancer 15:673. https://doi.org/10.1186/s12885-015-1679-x